frontiers in Earth Science

ORIGINAL RESEARCH
published: 09 April 2019
doi: 10.3389/feart.2019.00066

Internal Structures and Growth Style of a Quaternary Subaerial Rhyodacite Cryptodome at Ogariyama, Usu Volcano, Hokkaido, Japan

Yoshihiko Goto[1] and Akihiko Tomiya[2]**

[1] Muroran Institute of Technology, Muroran, Japan, [2] Geological Survey of Japan, National Institute of Advanced Industrial Science and Technology, Tsukuba, Japan

Cryptodomes are shallow-level intrusions that cause updoming of overlying sediments or other rocks. Understanding the formation of cryptodomes is important for hazard assessment, as cryptodome-forming eruptions are one of the major triggering factors in sector collapse. This paper describes internal structures of a Quaternary subaerial rhyodacite cryptodome at Ogariyama, Usu volcano, Japan (the Ogariyama dome), and examines the textural differences between subaerial and subaqueous cryptodomes to extend our knowledge of these phenomenon. The Ogariyama dome, which is one of the youngest subaerial cryptodomes in the world (<0.4 ka), can be viewed in cross-section because a vertical fault formed during the 1977–1978 eruption and cut through the center of the cryptodome, exposing its interior. The morphology of the cryptodome is scalene triangular in shape, with rounded corners in cross-section, and it is 150 m across and 80 m high. The internal structure of the dome is concentrically zoned, with a massive core, jointed rim, and brecciated border, all of which are composed of uniform, feldspar-phyric rhyodacite (SiO_2 = 71–72 wt.%). The massive core (130 m across) consists of coherent rhyodacite that has indistinct, large-scale flow banding and rectangular joints that are spaced 50–200 cm apart. The jointed rim (8–12 m wide) surrounds the massive core and consists of coherent rhyodacite that is characterized by distinct rectangular joints that are 30–80 cm apart and radiate outward. The outermost brecciated border (7–10 m wide) comprises monolithological breccia, consisting of angular rhyodacite clasts (5–30 cm across) and a cogenetic matrix. These internal structures suggest that the Ogariyama dome was formed by endogenous growth, involving continuous magma supply during a single intrusive event and simple expansion from its interior. The massive core formed by slow cooling of homogeneous rhyodacite magma. The jointed rim formed by fracturing of solidifying rhyodacite magma in response to cooling–contraction and dynamic stress driven by continued movement of the less viscous core. The brecciated border formed by fragmentation of the solidified rim of the dome in response to dynamic stress. The growth style of the Ogariyama dome closely resembles that of subaqueous cryptodomes. However, the morphology and internal structures of the Ogariyama dome differ from those of subaqueous cryptodomes, given its asymmetric morphology and absence of radial columnar joints

OPEN ACCESS

Edited by:
Guido Giordano, Università degli Studi Roma Tre, Italy

Reviewed by:
Thomas R. Walter, German Research Centre for Geosciences, Helmholtz Centre Potsdam, Germany
Claudio Antonio Tranne, University of Bologna, Italy

***Correspondence:**
Yoshihiko Goto
ygoto@mmm.muroran-it.ac.jp
Akihiko Tomiya
a.tomiya@aist.go.jp

Specialty section:
This article was submitted to Volcanology, a section of the journal Frontiers in Earth Science

Received: *30 July 2018*
Accepted: *14 March 2019*
Published: *09 April 2019*

Citation:
Goto Y and Tomiya A (2019) Internal Structures and Growth Style of a Quaternary Subaerial Rhyodacite Cryptodome at Ogariyama, Usu Volcano, Hokkaido, Japan. Front. Earth Sci. 7:66. doi: 10.3389/feart.2019.00066

and large-scale flow banding. These differences might reflect the well-consolidated and inhomogeneous physical properties of the host sediment and the slow cooling rate and high viscosity of the Ogariyama dome. The Ogariyama dome is probably the best cross-sectional example of a subaerial cryptodome in the world. Our descriptive study of the cryptodome provides invaluable information for hazard assessment.

Keywords: cryptodome, subaerial, rhyodacite, internal structure, endogenous growth

INTRODUCTION

Cryptodomes are shallow-level intrusions that cause updoming of overlying sediments or other rocks (Minakami et al., 1951; McPhie et al., 1993). They commonly form by the emplacement of silicic magma into poorly consolidated sediment (White et al., 2015). Cryptodomes are distinguished from lava domes in that magma does not appear on the ground surface. When a cryptodome partly breaks through the host sediment cover, the dome is termed a partly extrusive cryptodome (McPhie et al., 1993). Cryptodome-forming eruptions occur in both subaerial and subaqueous settings. The 1943–1945 eruption at Usu volcano, Hokkaido, Japan, produced the dacitic, partly extrusive cryptodome of Showa-Shinzan (Minakami et al., 1951; Mimatsu, 1962). The 1956 eruption at Bezymianny in Kamchatka produced a dacitic cryptodome during the pre-climactic stage, which led to a catastrophic sector collapse (e.g., Belousov, 1996). The 1980 eruption at Mount St. Helens in Washington, United States, also produced a dacitic cryptodome (bulge) on the volcano flank and caused a catastrophic sector collapse (e.g., Lipman et al., 1981; Voight et al., 1983). Marine geophysical studies of the Bay of Naples, Italy (Milia et al., 2012), suggest the presence of cryptodomes beneath the sea floor.

Understanding the formation of cryptodomes is important for hazard assessment and mineral exploration. Cryptodome-forming eruptions are one of the major triggering factors in sector collapse (e.g., Lipman et al., 1981; Voight et al., 1983; Siebert, 1984; Belousov, 1996; Riggs and Carrasco-Nunez, 2004). Cryptodome-forming eruptions cause ground deformation that is associated with major natural disasters (e.g., Mimatsu, 1962; Katsui et al., 1985; Ui et al., 2002). Submarine cryptodomes can be associated with the formation of volcanic-hosted massive sulfide deposits (e.g., Horikoshi, 1969; Allen, 1992; Allen et al., 1997; Doyle and McPhie, 2000). Internal fractures in submarine cryptodomes can be oil–gas reservoirs (e.g., the Katakai gas field, Japan; Yamada and Uchida, 1997; Nonaka et al., 2018).

Our knowledge of the nature and formation of cryptodomes remains limited. The morphology and internal structures of cryptodomes are poorly understood, because the silicic intrusions of most modern cryptodomes remain buried (e.g., the Usu-Shinzan dome in Japan; Katsui et al., 1985). Descriptive studies of the internal structures of cryptodomes have been based mainly on submarine examples in ancient successions (e.g., Horikoshi, 1969; Cas et al., 1990; Kurokawa, 1990; Allen, 1992; Hanson and Wilson, 1993; Hamasaki, 1994; Goto and McPhie, 1998; Doyle and McPhie, 2000; Stewart and McPhie, 2003; Páez et al., 2018). Few studies have provided detailed descriptions of the internal structures of subaerial cryptodomes (Goto et al., 2004; Mattsson et al., 2018).

A Quaternary subaerial cryptodome at Ogariyama, Usu volcano, southwestern Hokkaido, Japan, displays well-preserved primary internal structures in a cross-sectional exposure. The Ogariyama dome was emplaced within the amphitheater at the summit of the volcano during a historic eruption that occurred after AD 1663 (probably AD 1769 or 1822; Soya et al., 2007; Matsumoto and Nakagawa, 2011). The cross-section of this young cryptodome is visible because a vertical fault formed during the 1977–1978 eruption and cut through the center of the cryptodome, exposing its interior. The Ogariyama dome is probably the best cross-sectional example of a subaerial cryptodome in the world. A detailed description of the internal structures of the Ogariyama dome and comparison with previously reported, well-studied subaqueous cryptodomes might significantly extend our understanding of cryptodomes, as our knowledge of these structures is based mainly on subaqueous examples. The objectives of this research are to: (1) describe in detail the morphology and internal structures of the Ogariyama dome based on field mapping; (2) interpret the formation of the internal structures; (3) constrain the growth mode of the dome; and (4) compare the Ogariyama dome with subaqueous examples.

GEOLOGICAL SETTING

Usu is a post-caldera volcano of Toya caldera that is located at the junction between the Kuril and NE Japan arcs (**Figures 1A,B**). The edifice of Usu volcano rises 733 m above sea level and the volcano has a basal diameter of ∼6 km. It consists mainly of a basaltic to andesitic stratovolcano that is overlain by many silicic domes (**Figure 1C**; Yokoyama et al., 1973; Soya et al., 2007).

Previous geological studies (e.g., Soya et al., 2007; Goto et al., 2013; Goto and Danhara, 2018) suggest that the activity of Usu volcano commenced with an andesitic explosive eruption at 19–18 ka, followed by andesitic stratovolcano-building between 18 and 16 ka, and sector collapse at 16 ka. The sector collapse produced an amphitheater that is 1.5–2.0 km across at the summit of the stratovolcano (**Figure 1C**). Usu volcano was then dormant for ∼15 kyr. Eruptive activity of Usu volcano resumed with a rhyolitic Plinian eruption in AD 1663 (Yokoyama et al., 1973). Silicic dome-forming eruptions occurred in AD <1769, 1769, 1822, 1853, 1910, 1943–1945, 1977–1978, and 2000 (Tomiya and Miyagi, 2002; Ui et al., 2002; Nakagawa et al., 2005; Soya et al., 2007). These eruptions produced more than eleven

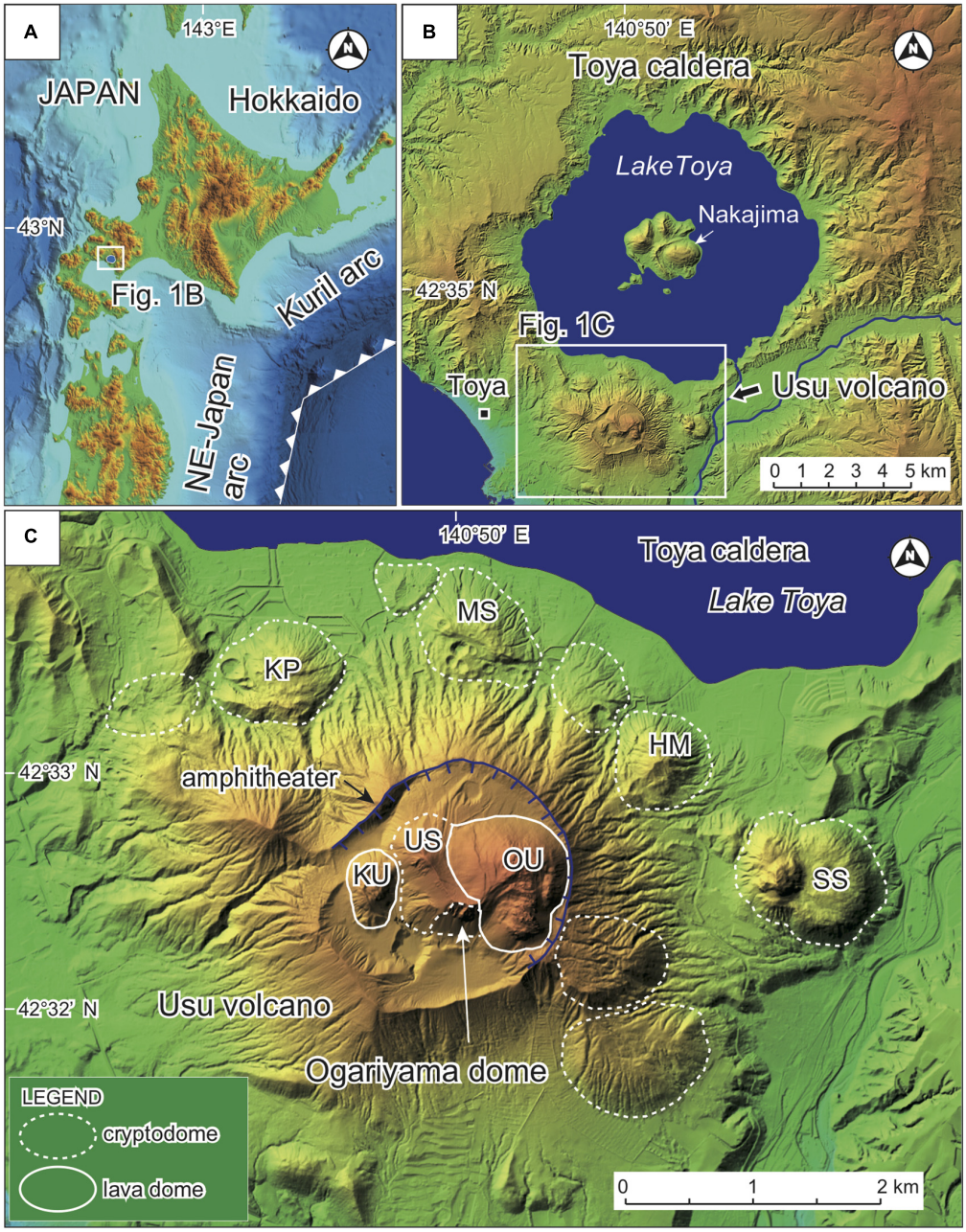

FIGURE 1 | (A) Tectonic setting of Usu volcano in southwestern Hokkaido, Japan. The volcano is located at the junction between the Kuril and NE Japan arcs. **(B)** Location of Usu volcano, which is a post-caldera volcano of Toya caldera. **(C)** Topographic map of Usu volcano, showing the location of the Ogariyama dome. Usu volcano comprises a basaltic to andesitic stratovolcano with an amphitheater at its summit, and contains many silicic cryptodomes and lava domes, including Kompira-yama (KP), Meiji-Shinzan (MS), Higashi-Maruyama (HM), Showa-Shinzan (SS), Ko-Usu (KU), Usu-Shinzan (US), O-Usu (OU), and Ogariyama. The base maps were produced by topographic data issued by the Geospatial Information Authority of Japan.

cryptodomes and two lava domes at the northern foot of the volcano and within the amphitheater (**Figure 1C**). Ogariyama is one of these cryptodomes and is located in the south–central part of the amphitheater (**Figure 1C**). The emplacement age of the Ogariyama cryptodome is considered to be AD 1769 based on petrological investigations (Matsumoto and Nakagawa, 2011), although Soya et al. (2007) suggested that the dome was emplaced in AD 1822. Its absolute emplacement age is unknown, as no historic documents have been found describing the dome growth. The word *Ogariyama* in Japanese means "growing mountain." Usu volcano is unique in terms of its frequency of cryptodome-forming eruptions (every 20–30 years; Soya et al., 2007). Such frequent cryptodome-forming eruptions can be attributed to the groundwater-rich environment of the volcano, which is located

nearby a caldera lake (Lake Toya; **Figure 1B**), and the intrusion of high-viscosity silicic magma during eruption.

Photographic records before AD 1977 (**Figure 2A**) indicate that the Ogariyama dome was a small mound ("roof mountain" of Mimatsu, 1962) standing on the amphitheater floor (Sobetsu Town, 2016). A topographic map published in 1975 (**Figure 3A**) indicates that the mound was 200–300 m across and 40 m high above the amphitheater floor. During the 1977–1978 eruption, large-scale ground deformation occurred within the amphitheater. The ground deformation was caused by the growth of a new cryptodome (Usu-Shinzan). Several east–west-trending faults appeared on the amphitheater floor (**Figures 2B**, **3A**), and some of these faults cut the Ogariyama dome into three parts (Katsui et al., 1985). The northernmost part of the Ogariyama dome was then gradually uplifted by ca. 180 m due to the growth of the Usu-Shinzan dome (**Figure 3B**). This uplift resulted in perfect exposure of the interior of the Ogariyama dome on the east–west-trending fault scarp along the southern perimeter of the Usu-Shinzan dome (**Figure 4**). Given that the fault vertically cut the Ogariyama dome through its center, a spectacular cross-section of the dome has been exhumed (**Figure 4**). During this ground deformation, volcaniclastic deposits on the amphitheater floor around the Ogariyama dome ("host sediment" of the Ogariyama dome) were also uplifted. The host sediment is presently exposed on the western side of the Ogariyama dome

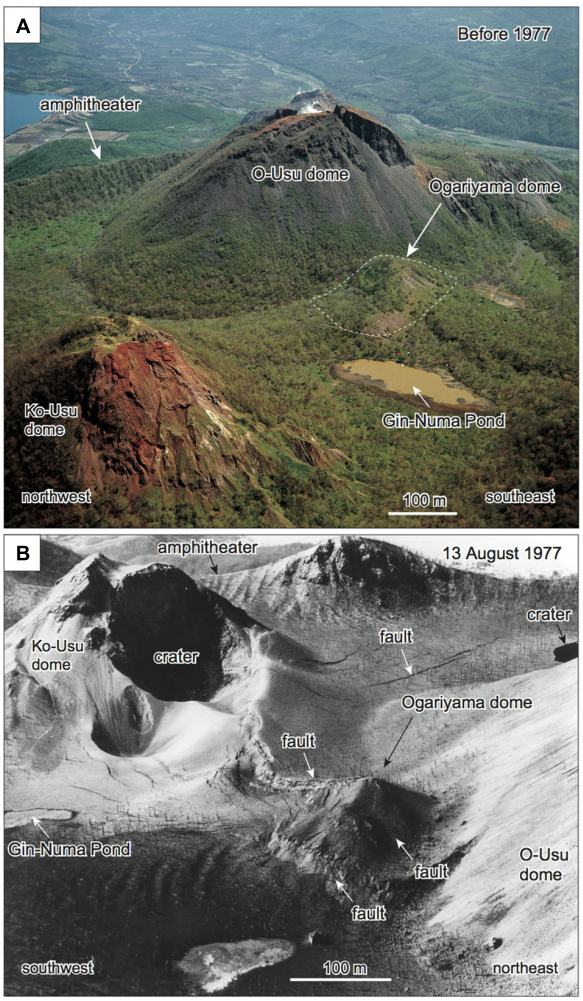

FIGURE 2 | (A) Aerial photograph of the Ogariyama dome, taken from the southwest before 1977. The photograph was provided by Toyako Town Office. **(B)** Aerial photograph of the Ogariyama dome taken from the southeast on 13 August 1977 (during the initial phase of the 1977–1978 eruption). Note that the Ogariyama dome is cut by several east–west-trending faults. The photograph (original black-and-white) was taken by Hokkaido Shinbun. The scale is approximate.

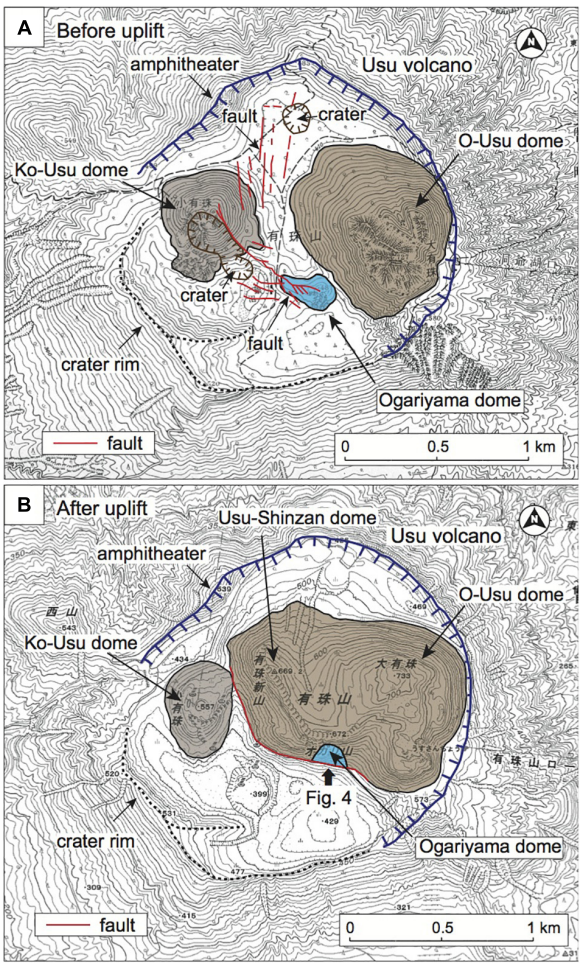

FIGURE 3 | (A) Topographic map of the summit area of Usu volcano before the 1977–1978 eruption, showing the location and shape of the Ogariyama dome before uplift. The Ogariyama dome is a small mound on the amphitheater floor. The base map was taken from a 1:25,000 scale topographic map issued in 1975 by the Geospatial Information Authority of Japan. Faults observed on 12 August 1977 (red lines) and craters that formed during the 1977 eruption (Katsui et al., 1985) are also shown. Note that the Ogariyama dome is cut by a fault. **(B)** Topographic map of the summit area of Usu volcano after the 1977–1978 eruption. The Ogariyama dome was cut by the fault, and its northern part was uplifted by the growth of the Usu-Shinzan cryptodome. The base map was taken from a 1:25,000 scale topographic map issued in 2008 by the Geospatial Information Authority of Japan.

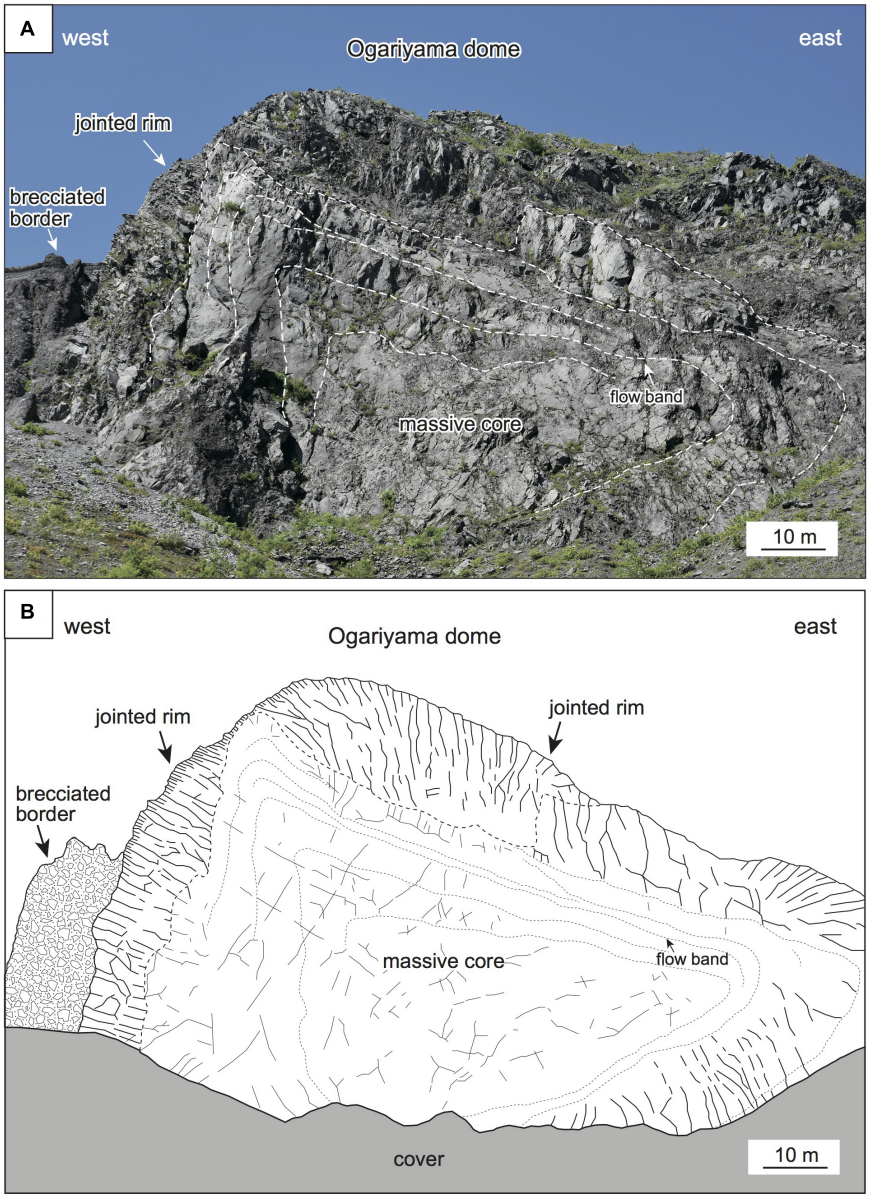

FIGURE 4 | (A) Photograph of a cross-section of the Ogariyama dome, viewed from the south. This cross-section is exposed on a fault scarp that formed in response to growth of the Usu-Shinzan cryptodome. A sketch of this outcrop is shown in **(B)**. The photograph was taken in 2018. **(B)** Sketch of the Ogariyama dome, viewed from the south. The Ogariyama dome has a scalene triangular shape, with rounded corners in cross-section, and is 150 m across and 80 m high. The Ogariyama dome is concentrically zoned, with a massive core, jointed rim, and brecciated border. The massive core comprises coherent rhyodacite that has indistinct, large-scale flow banding and poorly developed rectangular joints that are 50–200 cm apart. The jointed rim is characterized by many rectangular joints and irregular fractures. The brecciated border comprises monolithological breccia.

and is >50 m thick. It comprises rhyolitic to dacitic pyroclastic flow deposits, consisting of lithic clasts that are <50 cm in size set in a coarse-grained matrix, along with reworked deposits.

MATERIALS AND METHODS

Our geological survey of the Ogariyama dome focused on the morphology, internal structure, and lithology of the dome. A detailed field survey of the Ogariyama dome was undertaken in 2017 and 2018 at the outcrop along the fault scarp along the southern perimeter of the Usu-Shinzan dome (**Figure 4**). The outcrop is subvertical, >80 m high, and extends horizontally in an east–west direction for >1 km. The survey locations of the Ogariyama dome were dependent on accessibility. As the outcrop is a subvertical cliff, only the base of the outcrop was accessible (i.e., the middle to upper parts of the outcrop were inaccessible). Detailed descriptions and rock

sampling of the Ogariyama dome were therefore carried out along its base. We collected more than 50 rock samples from the outcrop.

The lithological characteristics of the Ogariyama dome were determined by: (1) digital microscopy (Keyence VHX-2000) observations of collected samples; (2) optical microscopy observations of thin-sections; (3) bulk density measurements of rock samples; and (4) whole-rock geochemical analysis. The digital microscopy was used for observations of millimeter-sized rock fragments collected from the dome margin. Optical microscopy was used to determine the texture and mineralogy of the rock samples collected from various locations in the dome. Point counting was used to determine the modal abundances of phenocrysts. The bulk densities of rock samples were measured by the glass bead method of Sasaki and Katsui (1981). Whole-rock major element data were obtained by X-ray fluorescence spectrometry (XRF; Rigaku ZSX-Primus-II) at Okayama University, Japan, following the methods described by Kimura and Yamada (1996).

RESULTS

The morphology, internal structure, and lithology of the Ogariyama dome are described below, based on our field surveys and laboratory analyses.

Morphology of the Ogariyama Dome

The Ogariyama dome has a scalene triangular shape with rounded corners in an east–west cross-section (**Figure 4**). The dome has a pointed top on its western side and a steep western slope that dips at 70°–80° and a gentle eastern slope that dips at 20°–30°. Therefore, the Ogariyama dome has an asymmetric (anisotropic) shape. The exposed dome is 150 m wide and 80 m high (**Figure 4**), which might largely represent the original size of the intrusive body of the cryptodome, because the fault cut the dome through its center. The contact between the Ogariyama dome and its host sediment is not exposed.

Internal Structure of the Ogariyama Dome

The internal structure of the Ogariyama dome is concentrically zoned parallel to the dome margin (**Figure 4**) and comprises: (1) a massive core; (2) a jointed rim; and (3) a brecciated border.

Massive Core

The massive core occupies most of the central part of the Ogariyama dome and is ∼130 m in diameter (**Figure 5A**). The core comprises pale gray, coherent (unbrecciated) rhyodacite with a uniform (homogeneous) texture (**Figure 5B**). The rhyodacite is dense and appears to be macroscopically non-vesicular, although it contains tiny cavities up to 0.1 mm across (described later). Indistinct, large-scale flow bands (Goto and McPhie, 1998; Stewart and McPhie, 2003) are present at the margin of the core (**Figure 5A**). The flow bands are approximately parallel to the outer surface of the core and comprise alternating darker and lighter bands, both of which range in thickness from 2 to 7 m. They show no systematic variation in thickness outward. Lithological differences between the darker and lighter bands are unknown because they are present in inaccessible parts of the outcrop. Similar banding has been reported from an experimentally simulated lava dome produced by the squeezing of viscous material (putty) through a narrow opening (Reyer, 1888). The massive core of the Ogariyama dome contains indistinct rectangular joints that overprint the flow bands. The joints are spaced at 50–200 cm intervals (**Figure 5B**). No columnar joints (i.e., prismatic joints with hexagonal or pentagonal outlines in cross-section) are present in the core.

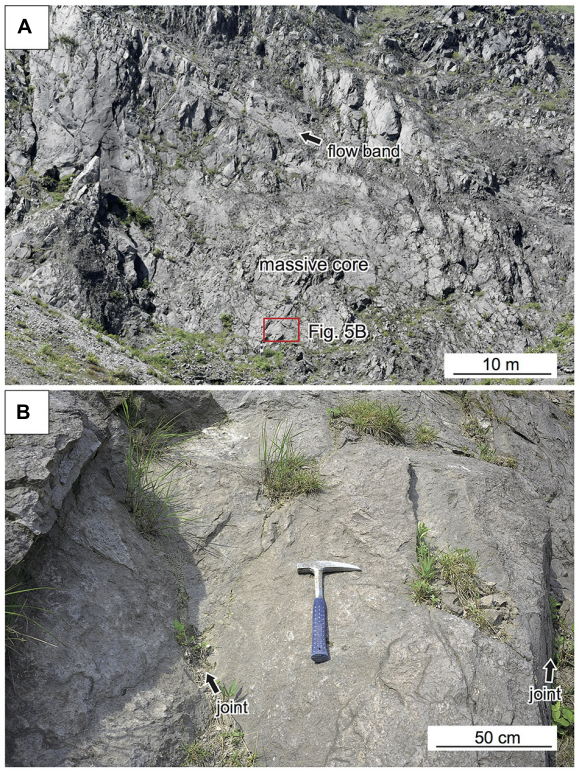

FIGURE 5 | (A) Photograph of the massive core of the Ogariyama dome. The location of **(B)** is indicated by the red rectangle. **(B)** Close-up view of the massive core of uniform rhyodacite. The hammer is 33 cm long.

The boundary between the core and jointed rim is distinct but gradual (**Figure 6A**). The core grades outward into the jointed rim and is marked by the appearance of a number of rectangular joints. Some joints in the core continue into the jointed rim. There is no glassy chilled contact (i.e., chilled margin) between the core and rim.

Jointed Rim

The jointed rim surrounds the core and is 8–12 m wide (**Figure 6A**). It comprises pale gray, coherent, uniform rhyodacite that contains many rectangular joints (**Figure 6B**). The rhyodacite is dense and appears to be macroscopically non-vesicular. No flow bands are visible in the rim. The rectangular

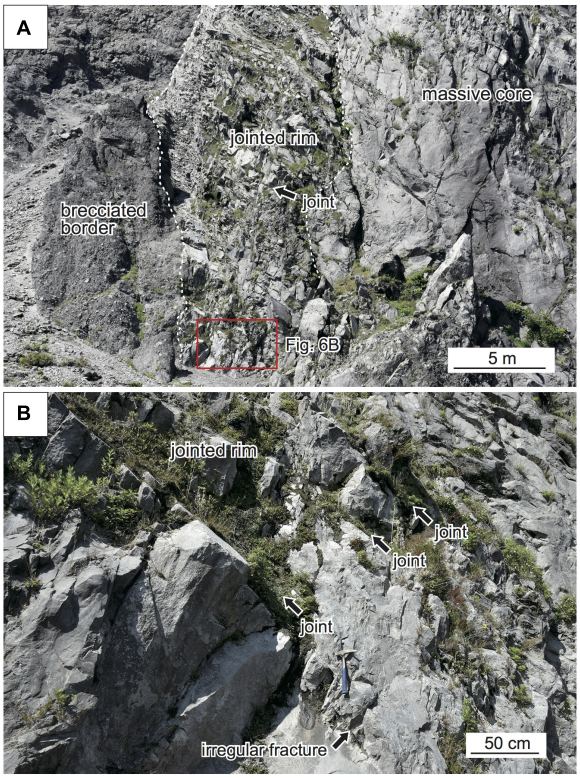

FIGURE 6 | (A) Photograph of the jointed rim of the Ogariyama dome, which occurs between the massive core and brecciated border. The location of **(B)** is indicated by the red rectangle. **(B)** Close-up view of the jointed rim, which contains numerous rectangular and parallel joints, as well as irregular fractures.

joints are approximately directed radially from the center to outer surface of the dome, but are not exactly perpendicular to the rim of the core (**Figure 6A**). The rectangular joints intersect the outer rim of the core at an angle of 60°–80° (**Figure 6B**). The rectangular joints are generally sub-parallel with a spacing of 30–80 cm, and gradually decrease in spacing outward. Each rectangular joint extends for 8–12 m through the rim and has a curved–planar surface. The rim also contains irregular fractures between the rectangular joints (**Figure 6B**). The irregular fractures have developed in random directions with a spacing of 10–30 cm. The surfaces of the irregular fractures are rough. There are no columnar joints in the rim.

The boundary between the rim and brecciated border is distinct but gradual (**Figure 6A**). There is no glassy chilled contact between the rim and border. Compared with the boundary between the core and rim, the boundary between the rim and border is more distinct.

Brecciated Border

The brecciated border occurs at the outermost part of the Ogariyama dome and is 7–10 m wide (**Figure 6A**). It comprises a gray, monolithological (monomict) breccia that consists of angular rhyodacite clasts that are 5–30 cm across set in a cogenetic matrix (**Figure 7A**). The breccia is massive (non-stratified), poorly sorted, and mostly shows a clast-rotated texture. Some domains also show a jigsaw texture. The clasts comprise more than 80 vol.% of the breccia. Each clast is a polyhedral rhyodacite fragment with sharp edges (**Figure 7A**). No glassy chilled margins were found on the clast surfaces. The rhyodacite of each clast is dense and macroscopically non-vesicular. The matrix of the breccia consists of angular rhyodacite fragments (<10 mm across) and fine ash (pulverized rhyodacite). Digital microscopy observations indicate that the rhyodacite fragments in the matrix have sharp edges (**Figure 7B**). Some small rhyodacite fragments (<1 mm across) have a flaky morphology (arrows in **Figure 7B**). There is no peperite (White et al., 2000; Skilling et al., 2002) within the brecciated border, suggesting that the host sediment was not fluidized during emplacement of the dome.

Lithology of the Ogariyama Dome

Texture and Mineral Assemblage

The rhyodacite of the massive core is uniformly porphyritic (**Figure 8A**). It contains euhedral plagioclase phenocrysts up to

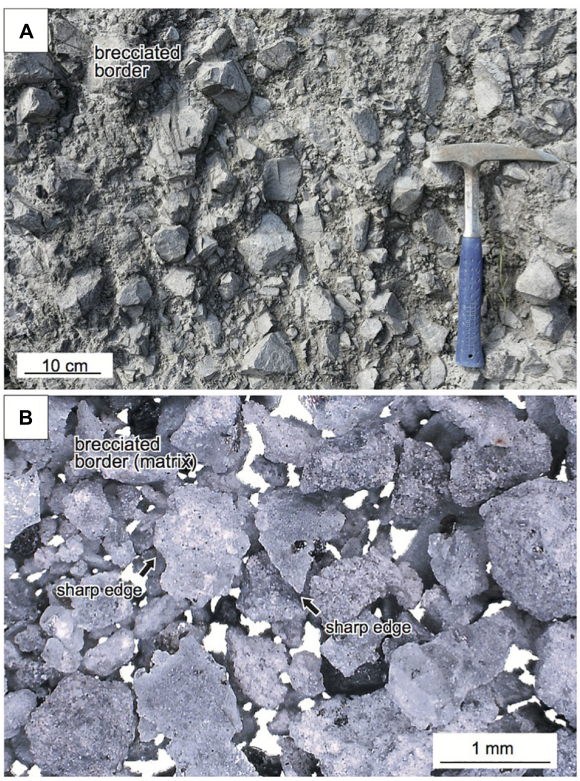

FIGURE 7 | (A) Photograph of the brecciated border of the Ogariyama dome, which comprises monolithological breccia consisting of angular rhyodacite clasts and a cogenetic matrix. **(B)** Close-up view of rhyodacite fragments in the matrix of the brecciated border. Some rhyodacite fragments have a flaky morphology with sharp edges (solid arrows). The photograph was taken with a digital microscope.

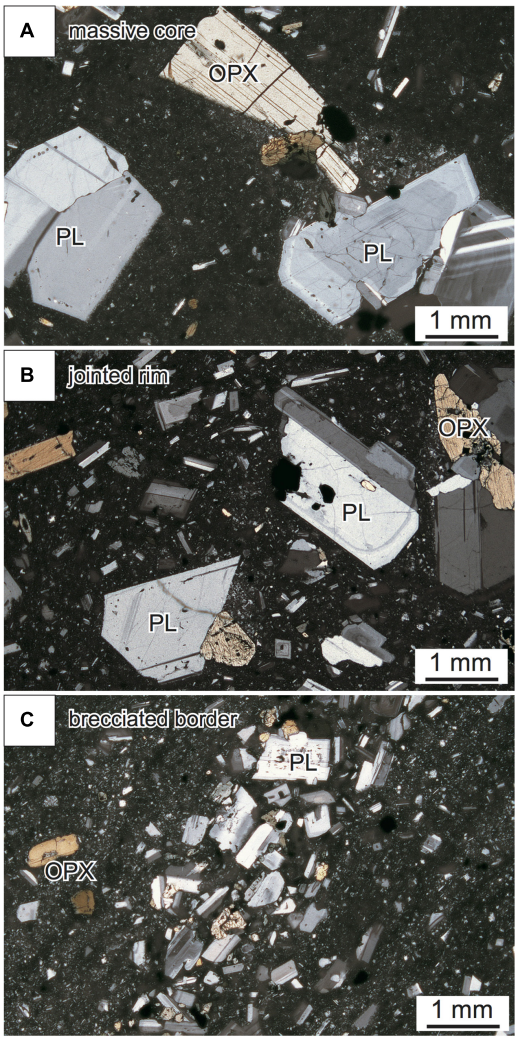

FIGURE 8 | Photomicrograph of rhyodacites from the **(A)** massive core, **(B)** jointed rim, and **(C)** brecciated border (cross-polarized light). Note that a phenocryst-rich zone occurs in the brecciated border. PL, plagioclase; OPX, orthopyroxene.

2 mm long (11–13 vol.% of the rhyodacite), hypersthene up to 2 mm long (1–2 vol.%), and opaque minerals up to 0.3 mm across (1 vol.%). Some phenocrysts are aggregated, forming "crystal clots" (Stewart, 1975) that are 1–3 mm across. The groundmass (~85 vol.%) of the rhyodacite has a microcrystalline texture and consists of plagioclase, hypersthene, silica minerals, and opaque minerals, all of which are up to 0.1 mm in size. Although no spherical vesicles are visible in the groundmass, irregularly shaped tiny cavities up to 0.1 mm across ("pores" of Zorn et al., 2018) occur sporadically among the crystals of the groundmass, in particular around the crystal clots.

The rhyodacite of the jointed rim is almost identical in terms of phenocryst assemblage, proportion, and size to the massive core (**Figure 8B**). It contains euhedral plagioclase phenocrysts up to 1.5–2.0 mm long (11–13 vol.%), hypersthene up to 2 mm long (1–2 vol.%), and opaque minerals up to 0.3 mm across (1 vol.%). However, the groundmass (~85 vol.%) of this rhyodacite is more glassy and has a hyalopilitic texture (Bates and Jackson, 1984; Allaby, 2008), consisting of plagioclase, hypersthene, and opaque minerals, all of which are up to 0.1 mm across, set in volcanic glass that has been partly devitrified. No or few cavities were visible in the groundmass.

The rhyodacite of the brecciated border differs in texture from those of the massive core and jointed rim (**Figure 8C**). The rhyodacite has a micro-banded texture that is characterized by numerous, parallel, phenocryst-rich zones. Each phenocryst-rich zone is 1–2 mm wide and they are spaced at 2–5 mm intervals. The phenocryst-rich zone consists of phenocrysts of plagioclase (<2 mm long), hypersthene (<1.5 mm long), and opaque minerals (<0.3 mm across). Most phenocrysts are euhedral, but some are fragmented. The total phenocryst proportion of this rhyodacite is almost identical to those of the massive core and fractured rim. The groundmass of the rhyodacite has a hyalopilitic texture, consisting of sub-parallel laths of plagioclase and hypersthene, granular opaque minerals (all <0.1 mm across), and volcanic glass. Although no spherical vesicles are visible in the groundmass, irregularly shaped cavities up to 0.5 mm across occur sporadically in the phenocryst-rich zone.

Density

Bulk densities were determined for rhyodacite samples collected from the massive core, jointed rim, and brecciated border. Samples locations are shown in **Figure 9**. A total of 75 rhyodacite samples were analyzed. The bulk density of the Ogariyama dome ranges from 2.0 to 2.6 g/cm^3 (**Figure 9**), which is consistent with the macroscopically non-vesicular texture of the three zones (cf. Zorn et al., 2018). The bulk densities of each zone are different. The massive core has the lowest bulk density (2.0–2.3 g/cm^3), the brecciated border has an intermediate density (2.1–2.5 g/cm^3), and the jointed rim has the highest density (2.4–2.6 g/cm^3).

Geochemistry

Whole-rock major element compositions of rhyodacites collected from the massive core (sample US-81), jointed rim (US-17), and brecciated border (US-80) were determined (**Table 1**). The analyzed samples are fresh (unaltered) rhyodacites. The rhyodacites from the three zones are compositionally uniform and contain 71.3–71.7 wt.% SiO_2, 14.7–14.9 wt.% Al_2O_3, 4.5–4.6 wt.% Na_2O, and 1.0 wt.% K_2O. Data for the rhyodacites plot on the boundary between the dacite and rhyolite fields in the total alkalis versus SiO_2 (TAS) diagram of Le Maitre et al. (1989) (**Figure 10**).

DISCUSSION

Environment of Dome Emplacement

The location and geology indicate that the Ogariyama dome was intruded into poorly consolidated volcaniclastic deposits that were emplaced within an amphitheater of an andesitic stratovolcano in a subaerial environment (**Figure 11A**). The absence of glassy chilled margins and peperites in the brecciated

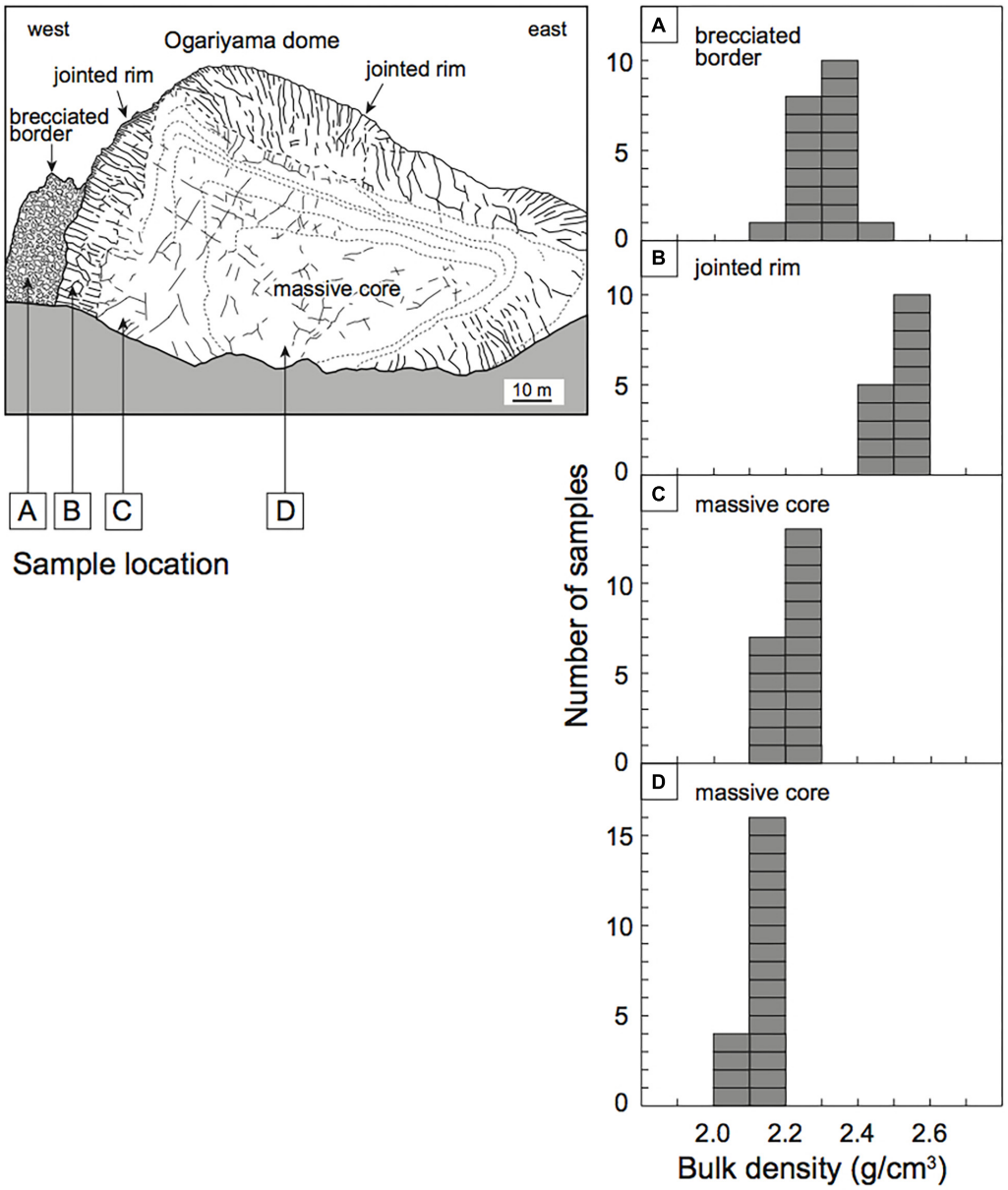

FIGURE 9 | Bulk densities of the rhyodacites from the **(A)** brecciated border, **(B)** jointed rim, and **(C,D)** massive core. Sampling positions **(A–D)** are shown in the sketch.

border demonstrates that the host sediment (i.e., volcaniclastic deposits) was not saturated with groundwater at the time of dome emplacement. However, we speculate that the host sediment contained some groundwater because photographic records (**Figure 2A**) show that a small pond (Gin-numa; 100–200 m across) was present on the amphitheater floor before the 1977–1978 eruption. No quantitative data are available to constrain the groundwater level at the time of dome emplacement, as no historic documents describe the growth of the Ogariyama dome. The morphology of the Ogariyama dome (i.e., not spherical; **Figure 4**) suggests that the cryptodome was not able to inflate in all directions, meaning it could not push away the surrounding host sediment in all directions. This intrusion behavior can be attributed to the relatively hard (and non-homogeneous) physical properties of the host sediment in a subaerial environment.

Origin of the Concentric Zones in the Ogariyama Dome

The Ogariyama dome is characterized by a concentrically zoned structure comprising a massive core, jointed rim, and brecciated border (**Figure 4**). These three zones are inferred to be genetically related internal structures that developed

TABLE 1 | Whole-rock major element data for rhyodacites from the massive core, jointed rim, and brecciated border of the Ogariyama dome.

	Massive core	Jointed rim	Brecciated border
Sample No.	**US-81**	**US-17**	**US-80**
SiO_2 (wt.%)	71.45	71.31	71.71
TiO_2	0.32	0.31	0.32
Al_2O_3	14.68	14.87	14.86
Fe_2O_3*	3.54	3.69	3.61
MnO	0.16	0.17	0.16
MgO	0.71	0.72	0.74
CaO	3.25	3.33	3.30
Na_2O	4.58	4.45	4.57
K_2O	1.03	1.00	1.02
P_2O_5	0.09	0.09	0.10
Total	99.81	99.94	100.39
L.O.I.	0.08	0.04	0.05

Fe_2O_3, total iron as Fe_2O_3. L.O.I., loss on ignition.*

within a single intrusion. They do not represent three discrete injections of magma, as the contacts between the zones are gradual. In addition, phenocryst mineralogy and abundances, and geochemical compositions are identical in all three zones, indicating the zones were produced from the same rhyodacite magma.

The massive core comprises mainly textually uniform (or weakly flow-banded) rhyodacite that has the widest joint intervals (<2 m apart) and highest groundmass crystallinity of the three zones. The spacing of cooling joints depends mainly on the rate of cooling (e.g., Grossenbacher and McDuffie, 1995), with slow cooling favoring more widely spaced joints. Groundmass crystallinity is also related to the rate of cooling, with slow cooling resulting in more complete crystallization. We thus infer that the massive core was formed by the slow cooling of relatively homogeneous rhyodacite magma.

The jointed rim comprises glassy rhyodacite that contains abundant rectangular joints in a zone surrounding the massive core, suggesting that they are syn-emplacement fractures. The rectangular joints have curved–planar surfaces, suggesting they formed in response to cooling–contraction (Kokelaar, 1986) and dynamic stress (Brooks et al., 1982; Kokelaar, 1986; Griffiths and Fink, 1993; Stewart and McPhie, 2003) in a viscous magma. The rectangular joints meet the outer rim of the massive core at an angle of 60°–80° (**Figure 6B**), indicating that dynamic stress played an important role in the joint formation. Therefore, we infer that the jointed rim was formed by the fracturing of solidifying rhyodacite magma around the massive core in response to cooling–contraction and dynamic stress due to continued movement of the less-viscous core of the actively growing dome (**Figure 11B**). During dome growth, both internal inflation and marginal shear might have occurred simultaneously in response to movement of the high-viscosity rhyodacite magma (**Figure 11A**). Similar syn-emplacement joints have been reported from a Miocene rhyolite cryptodome at Sandfell in Iceland (Mattsson et al., 2018).

The brecciated border is inferred to have formed by fragmentation of the rim of the cryptodome, as the rhyodacite clasts in the brecciated border are monolithological and lithologically identical to the jointed rim. Most rhyodacite clasts show a clast-rotated texture, suggesting that clasts of *in situ* breccia were rotated in response to shear stress due to continued movement of the less-viscous core. The angular morphology of the rhyodacite clasts (**Figure 7A**), absence of glassy chilled margins in the rhyodacite clasts, flaky rhyodacite fragments in the matrix (**Figure 7B**), and pulverized rhyodacite in the matrix all suggest that the brecciated border formed in response to dynamic stress (**Figure 11B**). Similar shear-induced breccia has been reported from the contact between the dacite intrusion (69 wt.% SiO_2) and host sediment of the Showa-Shinzan cryptodome (Goto et al., 2004). The phenocryst-rich zones in the rhyodacite clasts (**Figure 8C**) might have formed by strong shearing at the dome margins before fragmentation. Similar shear-induced textures have been reported from the marginal zone of dacitic lava spines at Mount St. Helens (Ryan et al., 2018).

Growth Style of the Ogariyama Dome

The growth style of volcanic domes is thought to be either endogenous, when a dome grows by internal inflation in response to the injection of new lava into the dome interior, or exogenous, when new lava is added to the outer surface of a dome (Fink et al., 1990; Fink, 1993; Calder et al., 2015). We infer that the growth style of the Ogariyama dome was endogenous.

The internal structure of the Ogariyama dome is concentric, suggesting that the dome formed by simple expansion in response to a continuous supply of magma during a single extrusive phase. A pulsating magma supply and multiple injections of magma separated in time would have resulted in a more complicated internal structure, comprising multiple domes or lobes with highly variable flow-banding orientations and a more complex arrangement of textural domains (e.g., Hamasaki, 1994; Závada et al., 2009).

The joint systems in the Ogariyama dome are consistent with endogenous growth. The rectangular joints in the massive core are spaced at intervals of 0.5–2.0 m, and those in the jointed rim at 0.3–0.8 m, suggesting that the isotherms (Spry, 1962) within the dome during cooling were concentric, which is consistent with endogenous inflation of the dome. Exogenous growth or multiple discrete injections of magma would have resulted in highly variable isotherms and more complicated joint patterns.

The bulk density in the three zones is also consistent with endogenous growth. The differences in bulk density among the three zones might reflect the variable porosity (i.e., the total volume of micro-size pores) of the rhyodacites, as the three zones have almost identical total phenocryst proportions and chemical compositions (**Table 1**). The lowest bulk density of the massive core might reflect the highest porosity of the three zones. The highest bulk density of the jointed rim might reflect the lowest porosity of the three zones. We infer that the lowest porosity of the jointed rim was due to rapid cooling of rhyodacite magma at the dome rim, whereas the highest porosity of the massive core reflects delayed vesiculation in the slowly cooling magma, caused

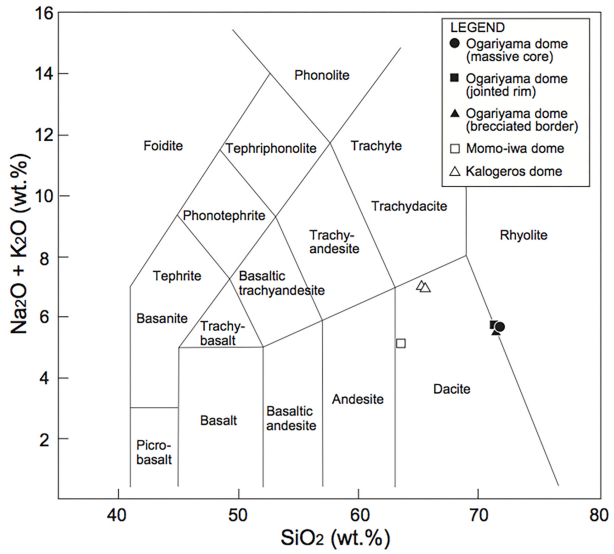

FIGURE 10 | Whole-rock chemical compositions of the Ogariyama dome plotted on the total alkalis versus SiO_2 (TAS) diagram of Le Maitre et al. (1989). Rhyodacites from the massive core (solid circle), jointed rim (solid square), and brecciated border (solid triangle) have identical chemical compositions and plot along the boundary between the dacite and rhyolite fields. Chemical compositions of the Momo-iwa dome in Japan (open square; Goto and McPhie, 1998) and the Kalogeros dome in Greece (open triangles; Stewart and McPhie, 2003) are also shown. All analytical data were recalculated to 100% on an H_2O (or loss on ignition) free basis.

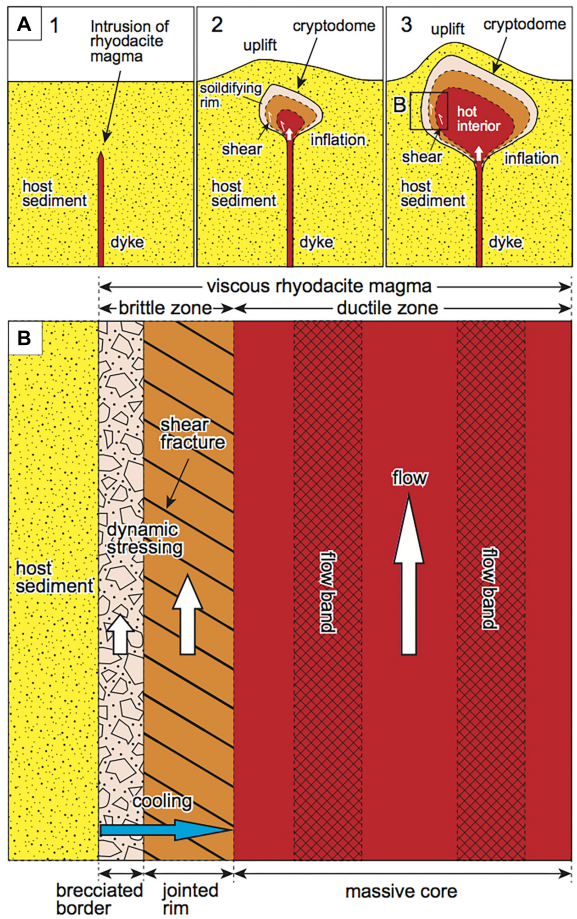

FIGURE 11 | (A) Schematic model of the growth of the Ogariyama dome, which has an asymmetric morphology. Internal inflation and marginal shear occurred simultaneously during dome growth. The location of the region shown in **(B)** is indicated by the rectangle. **(B)** Schematic model of the formation of the massive core, jointed rim, and brecciated border of the Ogariyama dome. The jointed rim and brecciated border formed in response to cooling–contraction and dynamic stress in a brittle zone.

by incomplete degassing during ascent due to the high magma viscosity (e.g., Sato et al., 1992).

Endogenous growth is a common growth style of subaqueous cryptodomes (Goto and McPhie, 1998; Stewart and McPhie, 2003; White et al., 2015). Both subaerial and subaqueous cryptodomes favor endogenous growth because they form by the emplacement of silicic magma into poorly consolidated sediment, which is deformed during dome growth.

Comparison With Subaqueous Examples

We now compare the morphology and internal structures of the Ogariyama dome with those of well-described subaqueous cryptodomes to extend our understanding of these structures. Examples of subaqueous cryptodomes have been reported by Goto and McPhie (1998) and Stewart and McPhie (2003). Goto and McPhie (1998) described a Miocene submarine dacite cryptodome at Momo-iwa, Rebun Island, Hokkaido, Japan. The Momo-iwa dome has a hemispheric morphology with a diameter of 200–300 m and height of 190 m. The internal structure of the dome is concentric, with a massive core, flow banded rim, and brecciated border. Radial columnar joints are well-developed from core to rim. Peperite occurs in the brecciated border. Stewart and McPhie (2003) described a Pliocene submarine dacite cryptodome at Kalogeros, Milos Island, Greece. The Kalogeros dome has a flattened hemispheric morphology with a diameter of 800–1300 m and height of 120 m. The internal structure of the dome is concentric, with a massive core, flow-banded rim, and brecciated border. The brecciated border comprises various types of breccias. Well-developed columnar joints occur from core to rim.

There are three differences between the Ogariyama dome and these subaqueous examples (**Figure 12**). The first difference is the asymmetric morphology of the Ogariyama dome, which has a scalene triangular shape, with rounded corners and a pointed top on its western side (**Figure 4**). In contrast, the morphology of submarine examples is simple, hemispherical, and symmetrical. This difference probably reflects the harder and non-homogeneous physical properties of the host sediments to the Ogariyama dome. The Ogariyama dome has an asymmetric (anisotropic) morphology because it was emplaced into relatively hard, non-water-saturated, coarse volcaniclastic deposits that were cut by faults or locally folded. Similar asymmetric morphologies of subaerial cryptodomes have been reported from the Showa-Shinzan

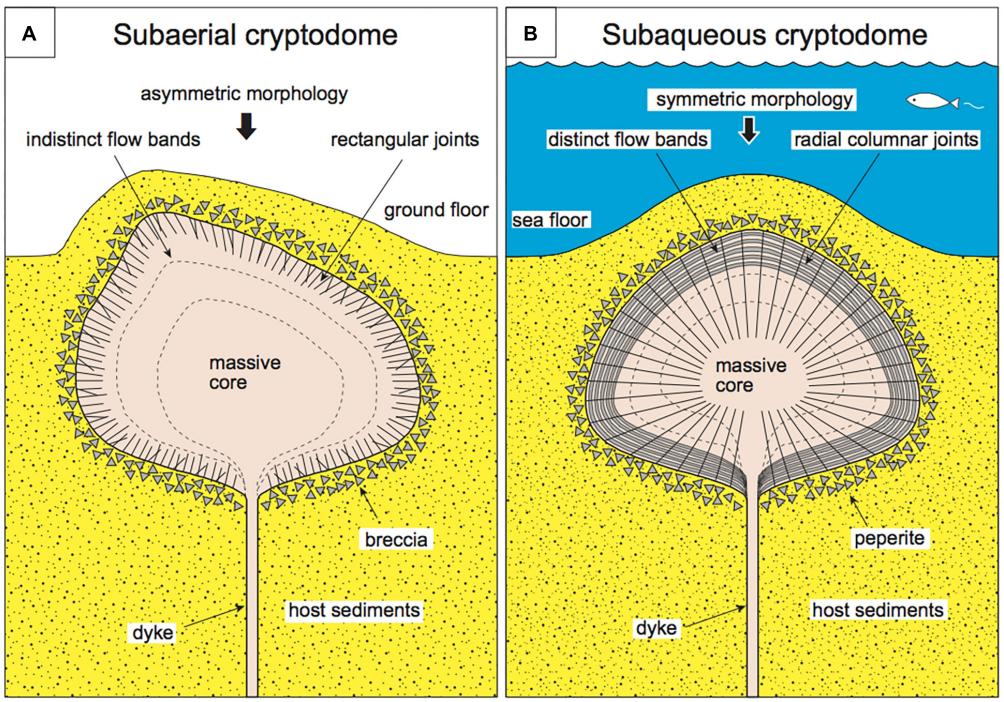

FIGURE 12 | Comparison between **(A)** a subaerial cryptodome and **(B)** a subaqueous cryptodome. The morphology and internal structures of the subaerial cryptodome differ from those of the subaqueous cryptodome. The subaerial cryptodome is characterized by an asymmetrical (anisotropic) morphology, distinct rectangular joints, and indistinct large-scale flow banding. The subaqueous cryptodome is characterized by a symmetrical morphology, well-developed radial columnar joints, and distinct large-scale flow banding. Peperite is only found in subaqueous cryptodomes.

cryptodome (e.g., Minakami et al., 1951; Mimatsu, 1962; Goto and Johmori, 2014) and Usu-Shinzan cryptodome (Katsui et al., 1985). Subaqueous cryptodomes typically have a simple, symmetrical, and hemispherical morphology because they are emplaced into water-saturated, isotropic, very soft mud, which is easily deformed and pushed away during the emplacement of a cryptodome.

The second difference is the absence of radial columnar joints in the Ogariyama dome. Subaqueous cryptodomes commonly have well-developed columnar joints (Goto and McPhie, 1998; Stewart and McPhie, 2003; White et al., 2015). This difference probably reflects the slow cooling of the Ogariyama dome. Columnar joints form in response to cooling–contraction (e.g., Spry, 1962), and column diameter depends mainly on the cooling rate, with slow cooling favoring more widely spaced joints (e.g., Grossenbacher and McDuffie, 1995). The high cooling rate of subaqueous cryptodomes results in well-developed columnar joints.

The third difference is the absence of distinct, large-scale flow banding in the Ogariyama dome, whereas such banding is commonly observed in subaqueous cryptodomes (Goto and McPhie, 1998; Stewart and McPhie, 2003; White et al., 2015). This difference possibly reflects the high viscosity of the Ogariyama dome. In general, silicic magma undergoes Bingham flow rather than Newtonian flow (e.g., Harris and Rowland, 2015). Bingham flow comprises a rigid plug at the core and shear zones along the margins. Flow banding forms in response to laminar shear in these shear zones (e.g., Cas and Wright, 1987). High-viscosity silicic magma is likely to behave as a rigid plug, which is not favorable for the development of flow bands. The Ogariyama dome has a higher SiO_2 content (71–72 wt.%) than the Momo-iwa dome (63 wt.%; Goto and McPhie, 1998) and Kalogeros dome (64–65 wt.%; Stewart and McPhie, 2003), indicating the higher viscosity of the former (**Figure 10**).

We propose that subaerial domes generally have higher viscosities than subaqueous domes because: (1) volcanic rocks in mature (continental) arcs have higher SiO_2 than those in immature (oceanic) arcs (e.g., Miyashiro, 1973); and (2) subaerial domes experience more complete degassing, resulting in a lower water content than subaqueous domes, as the confining pressure of subaerial domes is much lower than for subaqueous domes. The morphological and textural differences between the Ogariyama dome and subaqueous examples (i.e., the asymmetric morphology and the absence of well-developed radial columnar joints and large-scale flow banding in the Ogariyama dome) might reflect a combination of a harder host sediment, slower cooling rate, and higher viscosity of the Ogariyama dome. To our knowledge, the Ogariyama dome is the only example of a cross-sectional exposure of a Quaternary subaerial cryptodome worldwide. The dome provides a rare opportunity to study the primary internal structure of a subaerial cryptodome. Further case studies are required to better understand the textural differences between subaerial and subaqueous cryptodomes.

SUMMARY

The subaerial Ogariyama cryptodome on Usu volcano has a scalene triangular shape in cross-section and is 150 m across and 80 m high. The cryptodome has a concentric internal structure, with a massive core, jointed rim, and brecciated border. The massive core formed by slow cooling of homogeneous rhyodacite magma. The jointed rim formed by fracturing of solidifying rhyodacite magma in response to cooling–contraction and dynamic stress due to continued movement of the less-viscous core. The brecciated border formed by dynamic stress. Compared with subaqueous cryptodomes, the Ogariyama dome is characterized by an asymmetric morphology and absence of radial columnar joints and large-scale flow bands. These morphological and textural differences might reflect the harder host sediment, slower cooling rate, and higher viscosity of the Ogariyama dome.

AUTHOR CONTRIBUTIONS

YG contributed to the conception and design of this work, performed field surveys, and led the writing of the manuscript iteratively with AT. AT performed petrological investigations, advised YG on the geology of Usu volcano, and undertook revisions of the manuscript. YG and AT discussed and contributed to the final manuscript.

FUNDING

This work was supported by a grant from the Ministry of Education, Culture, Sports, Science and Technology of Japan (KAKENHI No. 16K05616 to AT) and the Muroran Institute of Technology (YG).

ACKNOWLEDGMENTS

We would like to thank H. Abe (Toya-Usu Geopark) for assistance with the geological field surveys. Toyako Town Office is thanked for providing a historic photograph. Hokkaido-Shinbun is thanked for allowing the use of an aerial photograph. Comments by the reviewers TW and CT, the editor GG, and the journal chief editor V. Acocella significantly improved the manuscript.

REFERENCES

Allaby, M. (2008). *A Dictionary of Earth Sciences*. New York, NY: Oxford University Press.

Allen, R. L. (1992). Reconstruction of the tectonic, volcanic and sedimentary setting of strongly deformed Zn-Cu massive sulfide deposits at Benambra, Victoria. *Econ. Geol.* 87, 825–854. doi: 10.2113/gsecongeo.87.3.825

Allen, R. L., Wihed, P., and Svenson, S. A. (1997). Setting of Zn-Cu-Au-Ag massive sulfide deposits in the evolution and facies architecture of a 1.9 Ga marine volcanic arc, Skellefte district, Sweden. *Econ. Geol.* 91, 1022–1053. doi: 10.2113/gsecongeo.91.6.1022

Bates, R. L., and Jackson, J. A. (1984). *Dictionary of Geological Terms*. Anchor Books: New York, NY.

Belousov, A. (1996). Deposits of the 30 March 1956 directed blast at Bezymianny volcano, Kamchatka, Russia. *Bull. Volcanol.* 57, 649–662. doi: 10.1007/s004450050118

Brooks, E. R., Wood, M. W., and Garbutt, P. L. (1982). Origin and metamorphism of peperite and associated rocks in the Devonian Elwell formation, northern Sierra Nevada, California. *Geol. Soc. Am. Bull.* 93, 1208–1231. doi: 10.1130/0016-7606(1982)93<1208:OAMOPA>2.0.CO;2

Calder, E. S., Lavallée, Y., Kendrick, J. E., and Bernstein, M. (2015). "Lava domes eruptions," in *Encyclopedia of Volcanoes*, 2nd Edn, ed. H. Sigurdsson (Amsterdam: Elsevier), 343–362. doi: 10.1016/B978-0-12-385938-9.00018-3

Cas, R. A. F., Allen, R. L., Bull, S. W., Clifford, B. A., and Wright, J. V. (1990). Subaqueous, rhyolitic dome-top tuff cones: a model based on the Devonian Bunga beds, southeastern Australia and a modern analogue. *Bull. Volcanol.* 52, 159–174. doi: 10.1007/BF00334802

Cas, R. A. F., and Wright, J. V. (1987). *Volcanic Successions: Modern and Ancient*. London: Allen and Unwin. doi: 10.1007/978-94-009-3167-1

Doyle, M. G., and McPhie, J. (2000). Facies architecture of a silicic intrusion-dominated volcanic centre at Highway-Reward, Queensland, Australia. *J. Volcanol. Geotherm. Res.* 99, 79–96. doi: 10.1016/S0377-0273(00)00159-1

Fink, J. H. (1993). "The emplacement of silicic lava flows and associated hazards," in *Active Lavas*, eds C. J. Kilburn and G. Luongo (London: University College London Press), 5–24.

Fink, J. H., Malin, M. C., and Anderson, S. W. (1990). Intrusive and extrusive growth of the Mount St. Helens lava dome. *Nature* 348, 435–437. doi: 10.1038/348435a0

Goto, Y., and Danhara, T. (2018). Tectonics, trigger, and timing of the catastrophic sector collapse at Usu volcano, Hokkaido, Japan. *Abstract Cities Volcanoes* 10:327.

Goto, Y., Ito, Y., Yokoyama, Y., Matsui, T., and Mimatsu, S. (2004). Internal structure of a subaerial dacite cryptodome at Usu volcano, Hokkaido, Japan. *Mem. Muroran Inst. Tech.* 54, 3–10.

Goto, Y., and Johmori, A. (2014). Resistivity structure of the Showa-Shinzan dome at Usu volcano, Hokkaido, Japan. *Bull. Volcanol. Soc. Japan* 59, 1–11. doi: 10.18940/kazan.59.1_1

Goto, Y., and McPhie, J. (1998). Endogenous growth of a Miocene submarine dacite cryptodome, Rebun Island, Hokkaido, Japan. *J. Volcanol. Geothrem. Res.* 84, 273–286. doi: 10.1016/S0377-0273(98)00040-7

Goto, Y., Sekiguchi, Y., Takahashi, S., Ito, H., and Danhara, T. (2013). The 18–19 ka andesitic explosive eruption at Usu volcano, Hokkaido, Japan. *Bull. Volcanol. Soc. Japan* 58, 529–541. doi: 10.18940/kazan.58.4_529

Griffiths, R. W., and Fink, J. H. (1993). Effects of surface cooling on the spreading of lava flows and domes. *J. Fluid Mech.* 252, 667–702. doi: 10.1017/S0022112093003933

Grossenbacher, K. A., and McDuffie, S. M. (1995). Conductive cooling of lava: columnar joint diameter and stria width as functions of cooling rate and thermal gradient. *J. Volcanol. Geothrem. Res.* 69, 95–103. doi: 10.1016/0377-0273(95)00032-1

Hamasaki, S. (1994). The internal structure of a rhyolite intrusion and the process of emplacement; an example from the Izumiyama porcelain stone deposit, Saga prefecture, southwestern Japan. *Bull. Volcanol. Soc. Japan* 39, 91–98.

Hanson, R. E., and Wilson, T. J. (1993). Large-scale rhyolitic peperites (Jurassic southern Chile). *J. Volcanol. Geotherm. Res.* 54, 247–264. doi: 10.1016/0377-0273(93)90066-Z

Harris, A. J. L., and Rowland, S. K. (2015). "Lava flows and rheology," in *Encyclopedia of Volcanoes*, 2nd Edn, ed. H. Sigurdsson (Amsterdam: Elsevier), 321–342. doi: 10.1016/B978-0-12-385938-9.00017-1

Horikoshi, E. (1969). Volcanic activity related to the formation of the Kuroko-type deposits in the Kosaka district, Japan. *Miner. Depos.* 4, 321–345. doi: 10.1007/BF00207161

Katsui, Y., Komuro, H., and Uda, T. (1985). Development of faults and growth of Usu-Shinzan cryptodome in 1977-1982 at Usu volcano, north Japan. *Journal Faculty Sci. Hokkaido Univ.* 21, 339–362.

Kimura, J., and Yamada, Y. (1996). Evaluation of major and trace element XRF analyses using a flux to sample ratio of two to one glass beads. *J. Mineral. Pet. Econo. Geol.* 91, 62–72. doi: 10.2465/ganko.91.62

Kokelaar, B. P. (1986). Magma–water interaction in subaqueous and emergent basaltic volcanism. *Bull. Volcanol.* 48, 275–289. doi: 10.1007/BF01081756

Kurokawa, A. (1990). Mode of occurrence and process of formation of subaqueous rhyolitic lavas in the Tadami province, Fukushima prefecture, Japan. *Earth Sci.* 44, 345–354.

Le Maitre, R. W., Bateman, P., Dudek, A., Keller, J., Lameyre Le Bas, M. J., Sabine, P. A., et al. (1989). *A Classification of Igneous Rocks and Glossary of Terms*. Oxford: Blackwell.

Lipman, P. W., Moore, J. G., and Swanson, D. A. (1981). Bulging of the north flank before the May 18 eruption: geodetic data. *US Geol. Surv. Prof. Pap.* 1250, 143–156.

Matsumoto, A., and Nakagawa, M. (2011). Formation history of lava domes at the summit of Usu volcano, Hokkaido, Japan, inferred from petrological features of the volcanic rocks. *Abstract Volcanol. Soc. Japan* 97, B2–B20.

Mattsson, T., Burchardt, S., Almqvist, B. S., and Ronchin, E. (2018). Syn-emplacement fracturing in the Sandfell laccolith, eastern Iceland—implications for rhyolite intrusion growth and volcanic hazards. *Front. Earth Sci.* 6:5. doi: 10.3389/feart.2018.00005

McPhie, J., Doyle, M., and Allen, R. (1993). *Volcanic Textures: A Guide to the Interpretation of Textures in Volcanic Rocks*. Hobart: Centre for Ore Deposit and Exploration Studies, University of Tasmania.

Milia, A., Torrente, M. M., and Bellucci, F. (2012). A possible link between faulting, cryptodomes and lateral collapses at Vesuvius Volcano (Italy). *Glob. Planet. Chang.* 90, 121–134. doi: 10.1016/j.gloplacha.2011.09.011

Mimatsu, M. (1962). *Showa-Shinzan Diary*. Hokkaido: Mimatsu Masao Memorial Museum, Sobetsu.

Minakami, T., Ishikawa, T., and Yagi, K. (1951). The 1944 eruption of Usu in Hokkaido, Japan. *Bull. Volcanol.* 11, 45–157. doi: 10.1007/BF02596029

Miyashiro, A. (1973). The Troodos ophiolitic complex was probably formed in an island arc. *Earth Planet. Sci. Lett.* 19, 218–224. doi: 10.1016/0012-821X(73)90118-0

Nakagawa, M., Matsumoto, A., Tajika, J., Hirose, W., and Ohtsu, T. (2005). Re-investigation of eruption history of Usu volcano, Hokkaido, Japan: finding of pre-Meiwa eruption (Late 17th century) between Kanbun (1663) and Meiwa (1769) eruptions. *Bull. Volcanol. Soc. Japan* 50, 39–52.

Nonaka, M., Sugiyama, Y., Ohtani, T., Yagi, M., and Yamada, Y. (2018). Facies architecture of a felsic subaqueous volcano in the Katakai gas field, Niigata, Japan. *Abstract Cities Volcanoes* 10:565.

Páez, G. N., Vidal, C. P., Galina, M., López, L., Jovic, S. M., and Guido, D. M. (2018). Intrusive hyaloclastite and peperitic breccias associated to sill and cryptodome emplacement on an Early Paleocene polymagmatic compound cone-dome volcanic complex from El guanaco mine, Northern Chile. *J. Volcanol. Geotherm. Res.* 354, 153–170. doi: 10.1016/j.jvolgeores.2018.02.011

Reyer, E. (1888). *Theoretische Geologie*. Stuttgart: E. Schweizerbart'sche Verlagshandlung.

Riggs, N., and Carrasco-Nunez, G. (2004). Evolution of a complex isolated dome system, Cerro Pizarro, central Mexico. *Bull. Volcanol.* 66, 322–335. doi: 10.1007/s00445-003-0313-y

Ryan, A. G., Friedlander, E. A., Russell, J. K., Heap, M. J., and Kennedy, L. A. (2018). Hot pressing in conduit faults during lava dome extrusion: Insights from Mount St. Helens 2004–2008. *Earth Planet. Sci. Lett.* 482, 171–180. doi: 10.1016/j.epsl.2017.11.010

Sasaki, T., and Katsui, Y. (1981). A new technique for measuring density of pumice using using glass beads. *Bull. Volcanol. Soc. Japan* 26, 117–118.

Sato, H., Fujii, T., and Nakada, S. (1992). Crumbling of dacite dome lava and generation of pyroclastic flows at Unzen volcano. *Nature* 360, 664–666. doi: 10.1038/360664a0

Siebert, L. (1984). Large volcanic debris avalanches: characteristics of source areas, deposits, and associated eruptions. *J. Volcanol. Geotherm. Res.* 22, 163–197. doi: 10.1016/0377-0273(84)90002-7

Skilling, I., White, J. D. L., and McPhie, J. (2002). *Peperites: Processes and Products of Magma-Sediment Mingling*. Amsterdam: Elsevier.

Sobetsu Town. (2016). *Living Together With the Active Volcano*. Sobetsu: Sobetsu Town office.

Soya, T., Katsui, Y., Niida, K., Sakai, K., and Tomiya, A. (2007). *Geological Map of Usu Volcano*, 2nd Edn. Tsukuba: Geol. Surv. Japan.

Spry, A. (1962). The origin of columnar jointing, particularly in basalt flows. *Geol. Soc. Aust. J.* 8, 191–216. doi: 10.1080/14400956208527873

Stewart, A. L., and McPhie, J. (2003). Internal structure and emplacement of an upper Pliocene dacitic cryptodome, Milos Island, Greece. *J. Volcanol. Geotherm. Res.* 124, 129–148. doi: 10.1016/S0377-0273(03)00074-X

Stewart, D. C. (1975). Crystal clots in calc-alkaline andesites as breakdown products of high-Al amphiboles. *Contrib. Mineral. Petrol.* 53, 195–204. doi: 10.1007/BF0037260

Tomiya, A., and Miyagi, I. (2002). The eruptive products and magma process of March 31, 2000 eruption of Usu volcano. *Bull. Volcanol. Soc. Japan* 47, 663–673.

Ui, T., Nakagawa, M., Inaba, C., Yoshimoto, M., Geological Party, and Joint Research Group for the Usu 2000 Eruption (2002). Sequence of the 2000 Eruption, Usu volcano. *Bull. Volcanol. Soc. Japan* 47, 105–117.

Voight, B., Janda, R. J., Glicken, H., and Douglass, P. M. (1983). Nature and mechanics of the Mount St. Helens rockslide-avalanche of 18 May 1980. *Geotechnique* 33, 243–273. doi: 10.1016/0148-9062(83)90666-6

White, J. D. L., McPhie, J., and Skilling, I. (2000). Peperite: a useful genetic term. *Bull. Volcanol.* 62, 65–66. doi: 10.1007/s004450050

White, J. D. L., McPhie, J., and Soule, S. A. (2015). "Submarine lavas and hyaloclastite," in *Encyclopedia of Volcanoes*, 2nd Edn, ed. H. Sigurdsson (Amsterdam: Elsevier), 363–375. doi: 10.1016/B978-0-12-385938-9.00019-5

Yamada, Y., and Uchida, T. (1997). Characteristics of hydrothermal alteration and secondary porosities in volcanic rock reservoirs, the Katakai gas field. *J. Japanese Assoc. Petrol. Technol.* 62, 311–320. doi: 10.3720/japt.62.311

Yokoyama, I., Katsui, Y., Oba, Y., and Ehara, Y. (1973). *Usuzan, Its Volcanic Geology, History of Eruption, Present State of Activity And Prevention of Disasters*. Sapporo: Committee for Prevention and Disasters of Hokkaido.

Závada, P., Kratinová, Z., Kusbach, V., and Schulmann, K. (2009). Internal fabric development in complex lava domes. *Tectonophysics* 466, 101–113. doi: 10.1016/j.tecto.2008.07.005

Zorn, E. U., Rowe, M. C., Cronin, S. J., Ryan, A. G., Kennedy, L. A., and Russell, J. K. (2018). Influence of porosity and groundmass crystallinity on dome rock strength: a case study from Mt. Taranaki, New Zealand. *Bull. Volcanol.* 80:35. doi: 10.1007/s00445-018-1210-8

Conflict of Interest Statement: The authors declare that the research was conducted in the absence of any commercial or financial relationships that could be construed as a potential conflict of interest.